Dislocation Type Evolution in Compressed Polycrystalline Nickel: Validation of Ashby's Model

Chaoyi Zhu*, Tyler Harrington*, Olivia Dippo*, George T. Gray III`, and Kenneth S. Vecchio*

*Department of NanoEngineering and Materials Science and Engineering Program, UC San Diego, La Jolla CA, 92131

`Los Alamos National Laboratory, Materials Science and Technology Division, Los Alamos, NM 87545

UC San Diego

Los Alamos NATIONAL LABORATORY EST. 1943

Dislocation Type: GND and SSD

Geometrically Necessary Dislocation

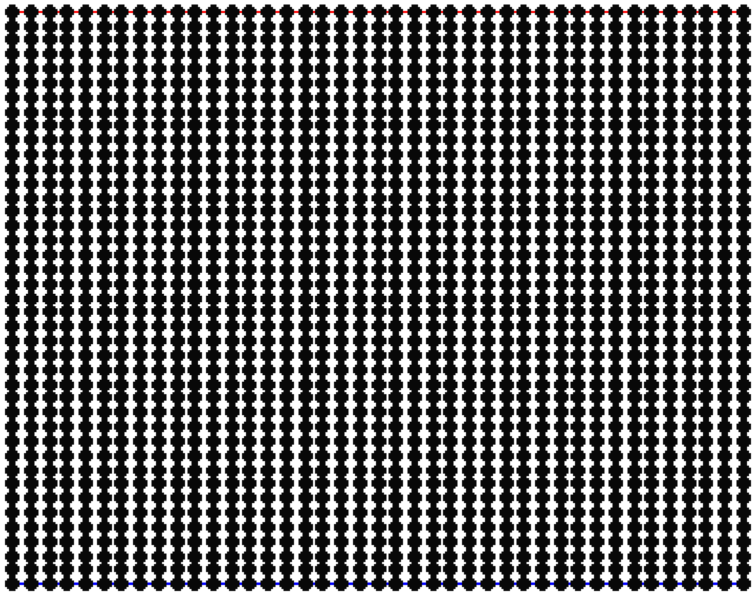

1. Accommodate lattice curvature associated with non-uniform deformation.
2. Obstacles to motions of SSD (work hardening).
3. Can be quantified in EBSD.

Statistically Stored Dislocation

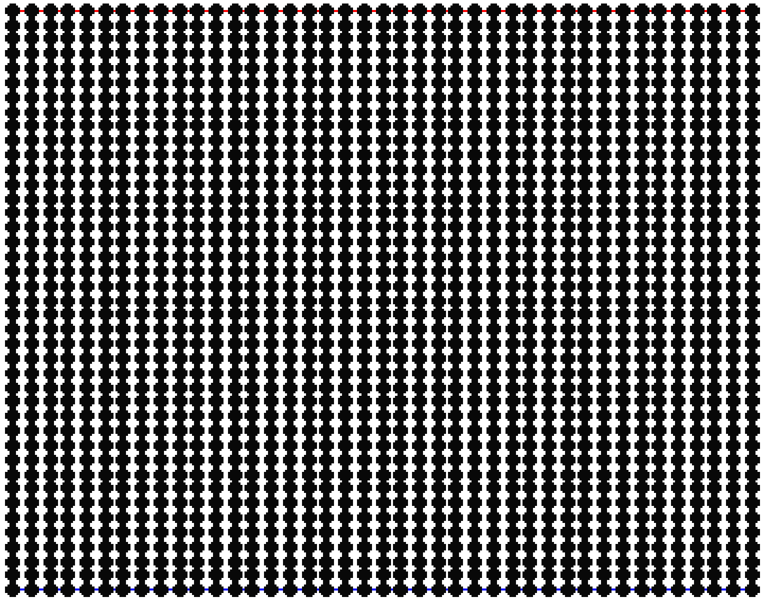

1. Generated due to random trapping process
2. Nucleation source for GNDs
3. Obstacles to motions of GND (work hardening)
4. Can not be quantified in EBSD

GND and SSD Evolution (Ashby)

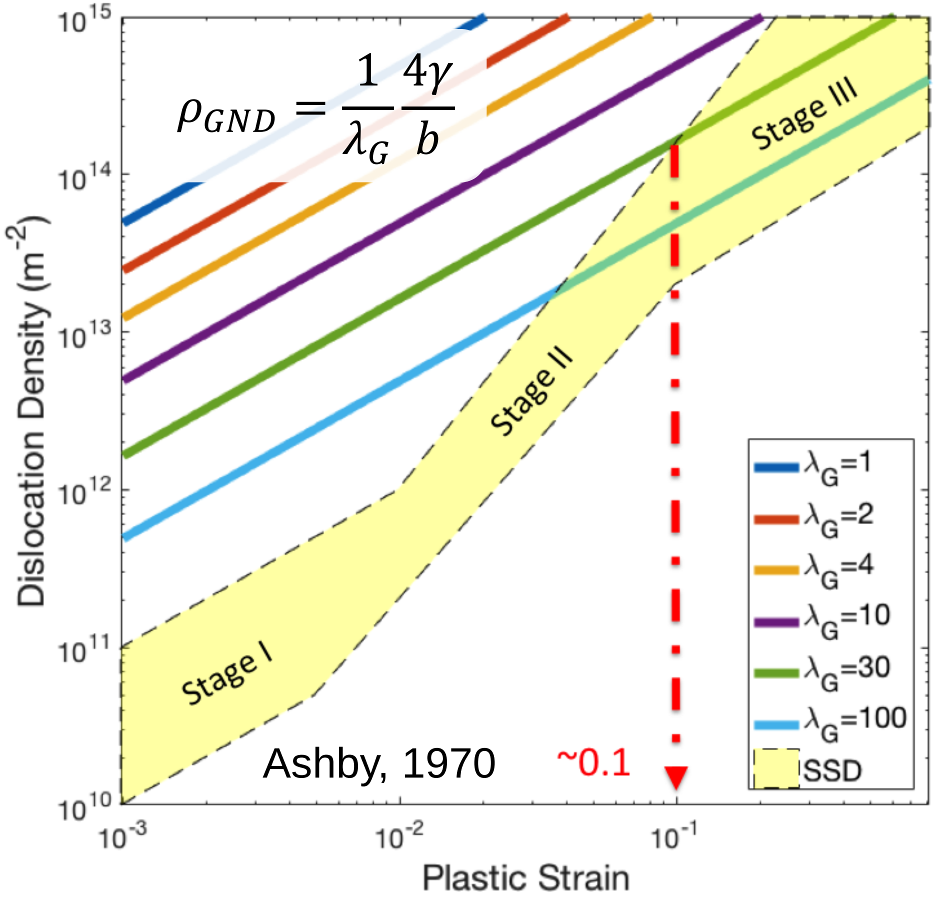

Correction of the materials overlap through GNDs

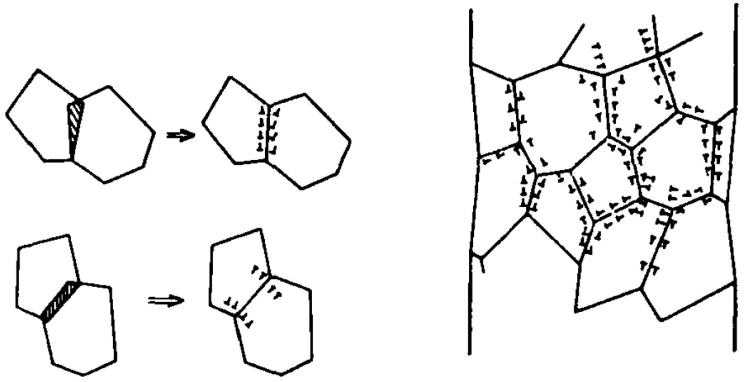

Ashby's model:

ρ_{GND}: microstructure (λ_G) and strain dependent (γ)

ρ_{SSD}: strain dependent (~ γ^2, measured in strained single crystal fcc crystal at room temperature by Basinski)

Grain size~30 μm, $\rho_{SSD} > \rho_{GND}$ at 0.1 strain

λ_G: average slip distance (~grain size)
γ: shear strain (Taylor's factor times compressive strain)
b: Burgers vector

Dislocation Density Tensor

- Fundamental equation: Nye dislocation density tensor $\boldsymbol{\alpha}$

$$\mathrm{B} = -\oint_{C} \beta^{pl} dx = -\oiint_{S} \nabla \times \beta^{pl} dS = \oiint_{S} \nabla \times \beta^{el} dS = \oiint \alpha dS$$

Stokes' theorem **Compatibility Demands**

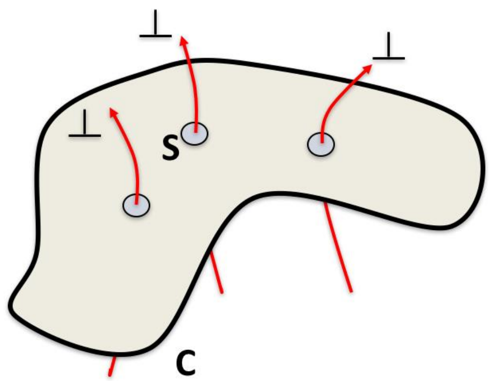

$$\boldsymbol{\alpha} = \boldsymbol{\nabla} \times \boldsymbol{\beta}^{el}$$

$\nabla \times$: curl operator

β^{el}: elastic distortion tensor

Dislocation density tensor describes the dislocation flux through the surface S.

Nye, 1953

Dislocation Density Tensor

- Nye tensor under infinitesimal elastic strain assumption

$$\alpha_{i\gamma} = \epsilon_{\alpha\beta\gamma}\beta^{el}_{i\alpha,\beta} = \epsilon_{\alpha\beta\gamma}\omega_{i\alpha,\beta} + \epsilon_{jlk}\varepsilon_{ij,l} \approx \epsilon_{\alpha\beta\gamma}\omega_{i\alpha,\beta} \approx \epsilon_{\alpha\beta\gamma}\Delta\emptyset_{i\alpha,\beta}$$

$$\boldsymbol{\alpha} \approx \begin{bmatrix} \frac{\partial\omega_{12}}{\partial x_3} - \frac{\partial\omega_{13}}{\partial x_2} & \frac{\partial\omega_{13}}{\partial x_1} & \frac{\partial\omega_{21}}{\partial x_1} \\ \frac{\partial\omega_{32}}{\partial x_2} & \frac{\partial\omega_{23}}{\partial x_1} - \frac{\partial\omega_{21}}{\partial x_3} & \frac{\partial\omega_{21}}{\partial x_2} \\ \frac{\partial\omega_{32}}{\partial x_3} & \frac{\partial\omega_{13}}{\partial x_3} & \frac{\partial\omega_{31}}{\partial x_2} - \frac{\partial\omega_{32}}{\partial x_1} \end{bmatrix}$$

ω: lattice rotation matrix
$\Delta\emptyset$: disorientation matrix

Latin: crystal coordinates
Greek: sample coordinates

Elastically rigid plastic approximation: inhomogeneous plastic distortion of the lattice is fully accommodated by the elastic lattice rotation alone. **B.C. Larson *et al*., 2007**

Measuring Lattice Orientation Gradient

- **Orientation gradient in the sample surface normal direction is inaccessible in 2D-EBSD**

$$\boldsymbol{\alpha} \approx \begin{bmatrix} \frac{\partial \omega_{12}}{\partial x_3} - \frac{\partial \omega_{13}}{\partial x_2} & \frac{\partial \omega_{13}}{\partial x_1} & \frac{\partial \omega_{21}}{\partial x_1} \\ \frac{\partial \omega_{32}}{\partial x_2} & \frac{\partial \omega_{23}}{\partial x_1} - \frac{\partial \omega_{21}}{\partial x_3} & \frac{\partial \omega_{21}}{\partial x_2} \\ \frac{\partial \omega_{32}}{\partial x_3} & \frac{\partial \omega_{13}}{\partial x_3} & \frac{\partial \omega_{31}}{\partial x_2} - \frac{\partial \omega_{32}}{\partial x_1} \end{bmatrix}$$

- **Frame of reference**: the lattice orientation gradient $\Delta\emptyset_{i\alpha,\beta}$ needs to be in the **sample frame,** same as the scan step

$$\Delta\phi_{dis} = \min\{\cos^{-1}\{tr[O_j^{cry}\mathbf{g}_B)(O_i^{cry}\mathbf{g}_A)^{-1}]\}\}$$

$$\Delta\emptyset_{i\alpha,\beta} \approx \frac{[(O_j^{cry}\mathbf{g}_B)(O_i^{cry}\mathbf{g}_A)^{-1} - I]\mathbf{g}_A}{scan\ step}$$

Electron Backscatter Diffraction

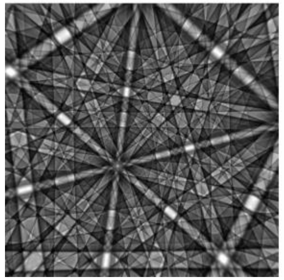

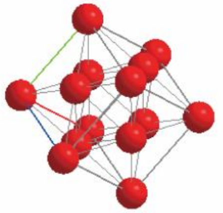

Dislocation Density Calculation

- Consistency in coordinates system is required, Wheeler *et al*, 2009

$$\alpha_{\alpha\gamma} \approx \mathbf{g}_{\alpha i}(\epsilon_{\boldsymbol{\alpha\beta\gamma}}\Delta\emptyset_{\boldsymbol{i\alpha,\beta}}) \qquad \alpha_{\alpha\gamma} = \sum_{n=1}^{N} \rho_{GND}^{n} b_{\alpha}^{n} \hat{l}_{\gamma}^{n}$$

- Solve for the dislocation density vector ρ :

$$\boldsymbol{\xi}(\mathbf{6}\times\mathrm{N})\cdot\boldsymbol{\rho}(\mathbf{N}\times\mathbf{1}) = \boldsymbol{\Lambda}(\mathbf{6}\times\mathbf{1})$$

$$\begin{pmatrix} b_1^1 l_1^1 - \frac{1}{2}\boldsymbol{b}^1\cdot\boldsymbol{l}^1, \cdots, b_1^N l_1^N - \frac{1}{2}\boldsymbol{b}^{\boldsymbol{N}}\cdot\boldsymbol{l}^{\boldsymbol{N}} \\ b_1^1 l_2^1, \cdots, b_1^N l_2^N \\ b_1^1 l_3^1, \cdots, b_1^N l_3^N \\ b_2^1 l_1^1, \cdots, b_2^N l_1^N \\ b_2^1 l_2^1 - \frac{1}{2}\boldsymbol{b}^1\cdot\boldsymbol{l}^1, \cdots, b_2^N l_2^N - \frac{1}{2}\boldsymbol{b}^{\boldsymbol{N}}\cdot\boldsymbol{l}^{\boldsymbol{N}} \\ b_2^1 l_3^1, \cdots, b_2^N l_3^N \end{pmatrix} \begin{pmatrix} \rho_1 \\ \vdots \\ \rho_N \end{pmatrix} = \begin{pmatrix} \frac{1}{2}\boldsymbol{T}(\boldsymbol{\alpha}) - \alpha_{11} \\ -\alpha_{12} \\ -\alpha_{13} \\ -\alpha_{21} \\ \frac{1}{2}\boldsymbol{T}(\boldsymbol{\alpha}) - \alpha_{22} \\ -\alpha_{23} \end{pmatrix}$$

Britton and Wilkinson, 2012

- N>6: L1 dislocation energy minimization scheme ($E_{edge}=E_{screw}/(1-v)$, v is the Poisson's ratio):

$$minimum\left\{E_{GND,total}^{L^{1e}} = \boldsymbol{E}_{\boldsymbol{N}}\cdot\boldsymbol{\rho} \mid \boldsymbol{\xi}' \subset \boldsymbol{\xi}, \boldsymbol{\Lambda} = \boldsymbol{\xi}'\cdot\boldsymbol{\rho}\right\}$$

Measurement Resolution (Lower Limit)

- Angular resolution of EBSD is between 0.2°~1°
- Resolution of GND measurement is limited by angular resolution and step size
- Noise floor:

$$\rho_{\mathrm{GND}}^{\mathrm{res}} = \frac{\text{Angular Resolution (rad)}}{\text{Step size (m)} \times \text{Burgers vector(m)}}$$

Humphreys et al, 2001
Wilkinson and Randman, 2010

Measurement Resolution (Upper Limit)

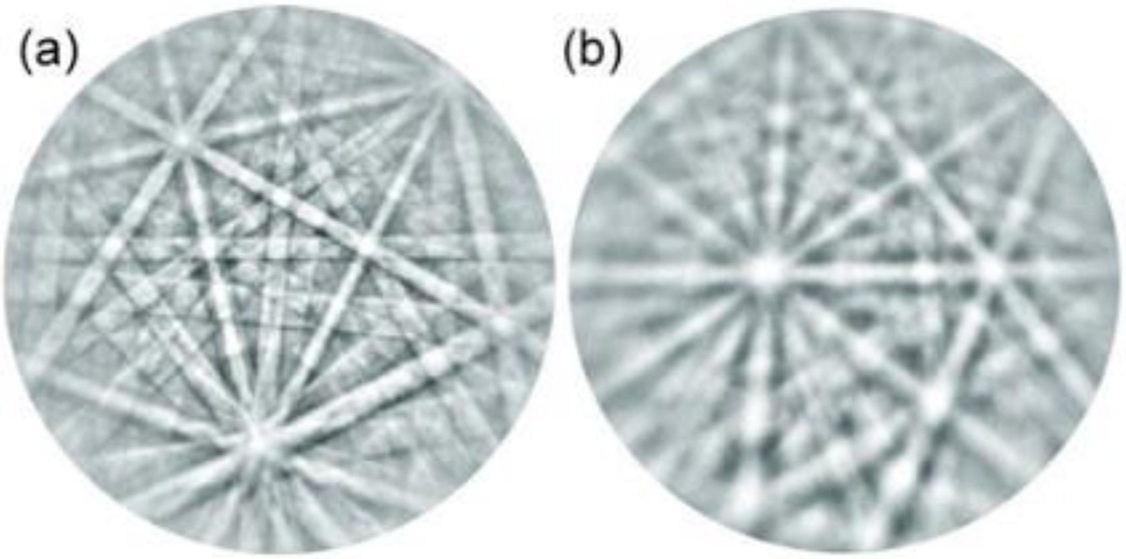

Pattern degradation due to severe plastic deformation.

Wright *et al.*, 2011

Appropriate Step Size (Burgers Circuit Size)

- L>> average spacing between dislocations $(1/\sqrt{\rho_{GND}})$
- L<< length scale over which there is significant variation in the plastic deformation field $(1/b \cdot \rho_{GND})$

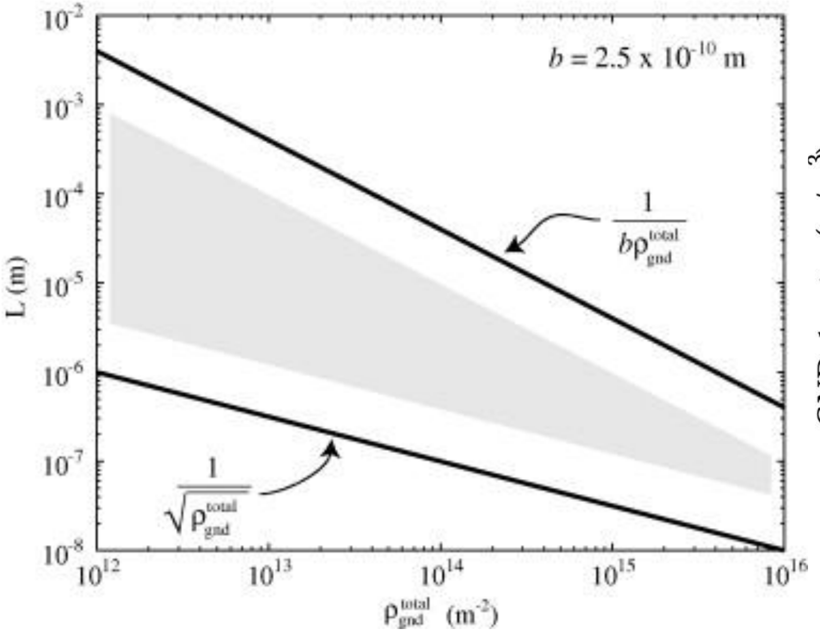

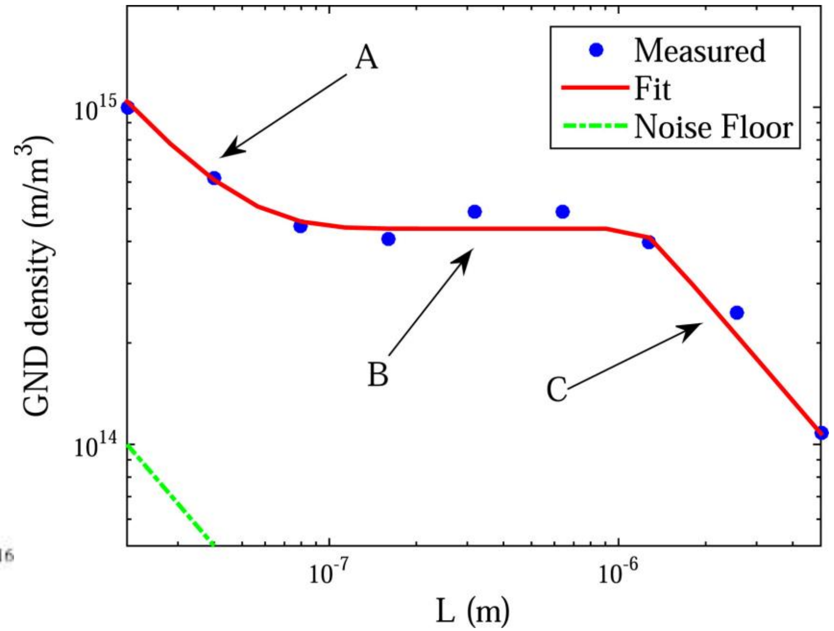

A: Overestimate (<100 nm)

B: 'true' density (100 nm~1μm)

C: Underestimate (>1μm)

Kysar *et al*., 2010
Ruggles *et al*., 2016

Material Fabrication and Characterization

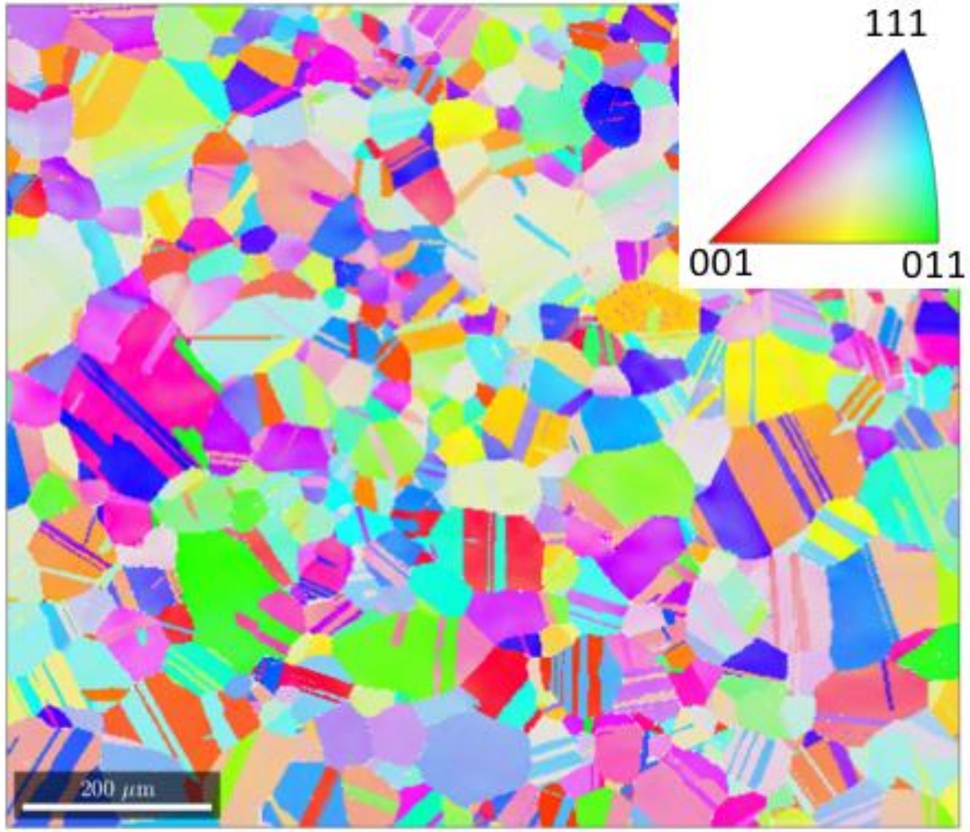

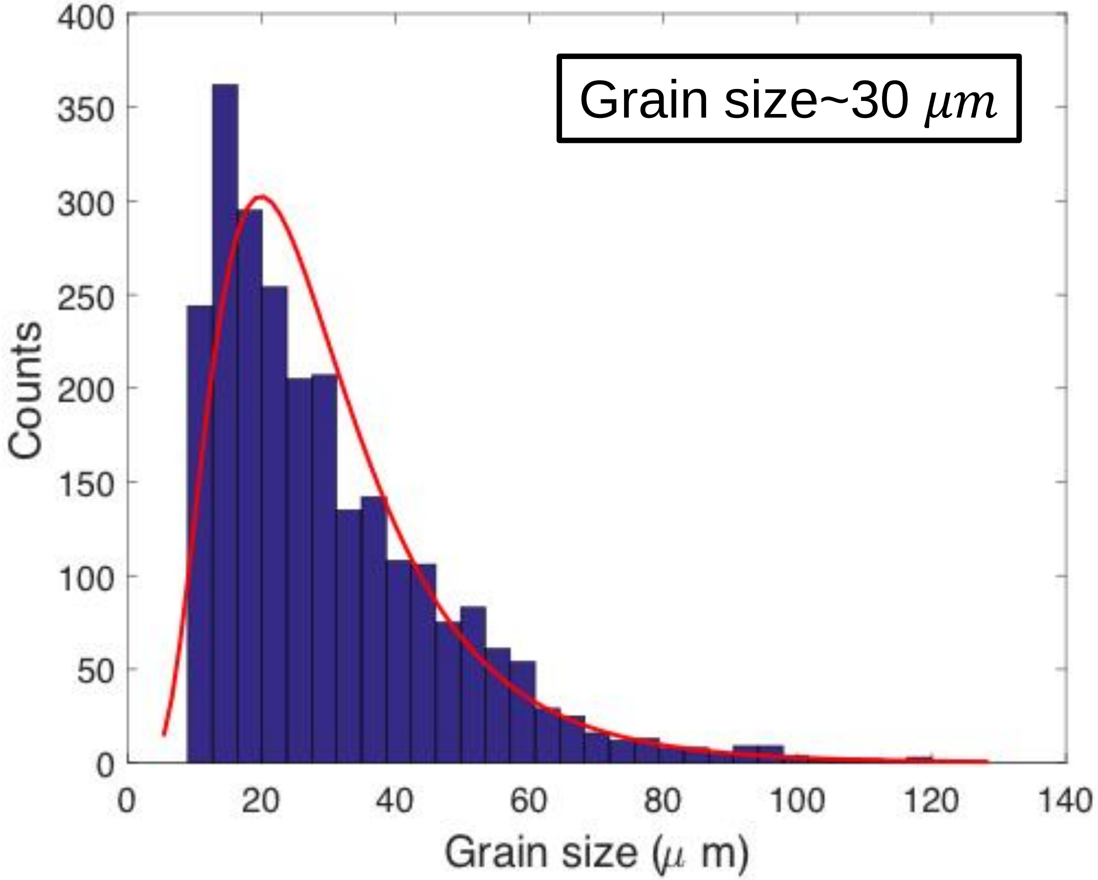

Nickel powder SPS 1200°C under a 50 MPa uniaxial load for a 5-minute hold and then annealed (~99% density)

Zhu *et al*, Acta Materialia, 2018

Materials and Sample Preparation

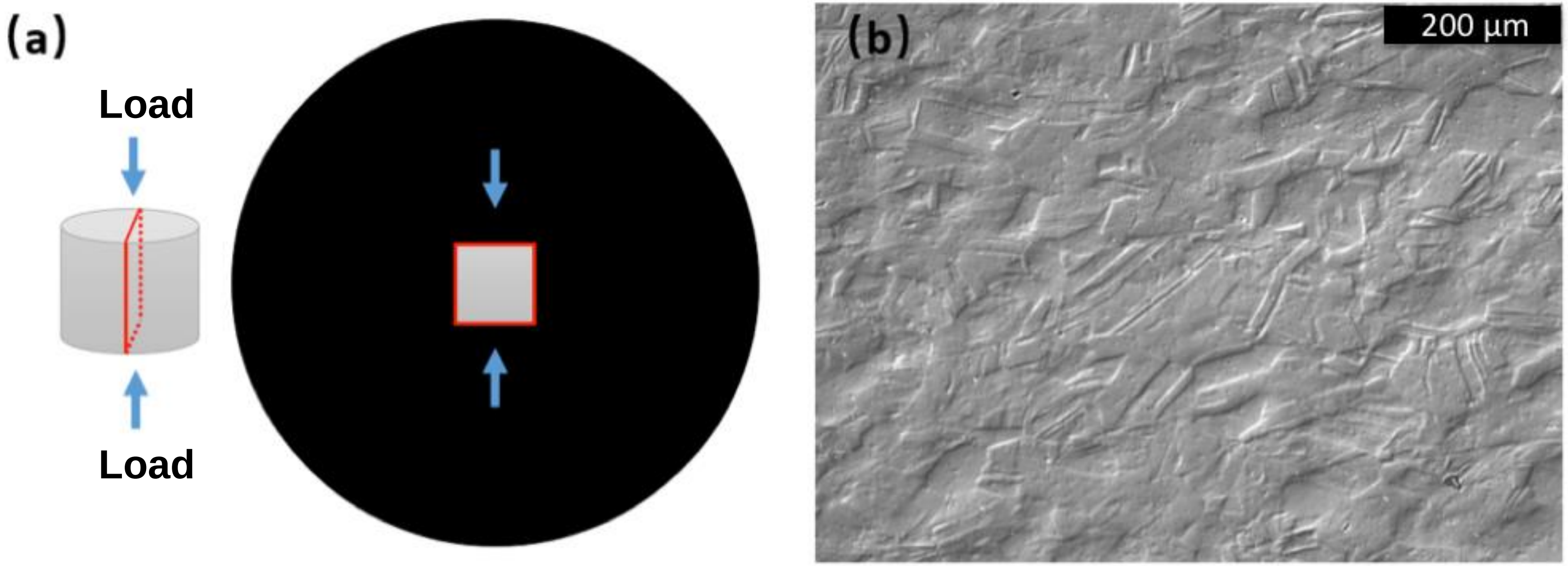

3 mm by 3 mm cylinder

EBSD Scans

Imposed plastic strain varying from 0.05 to 0.46

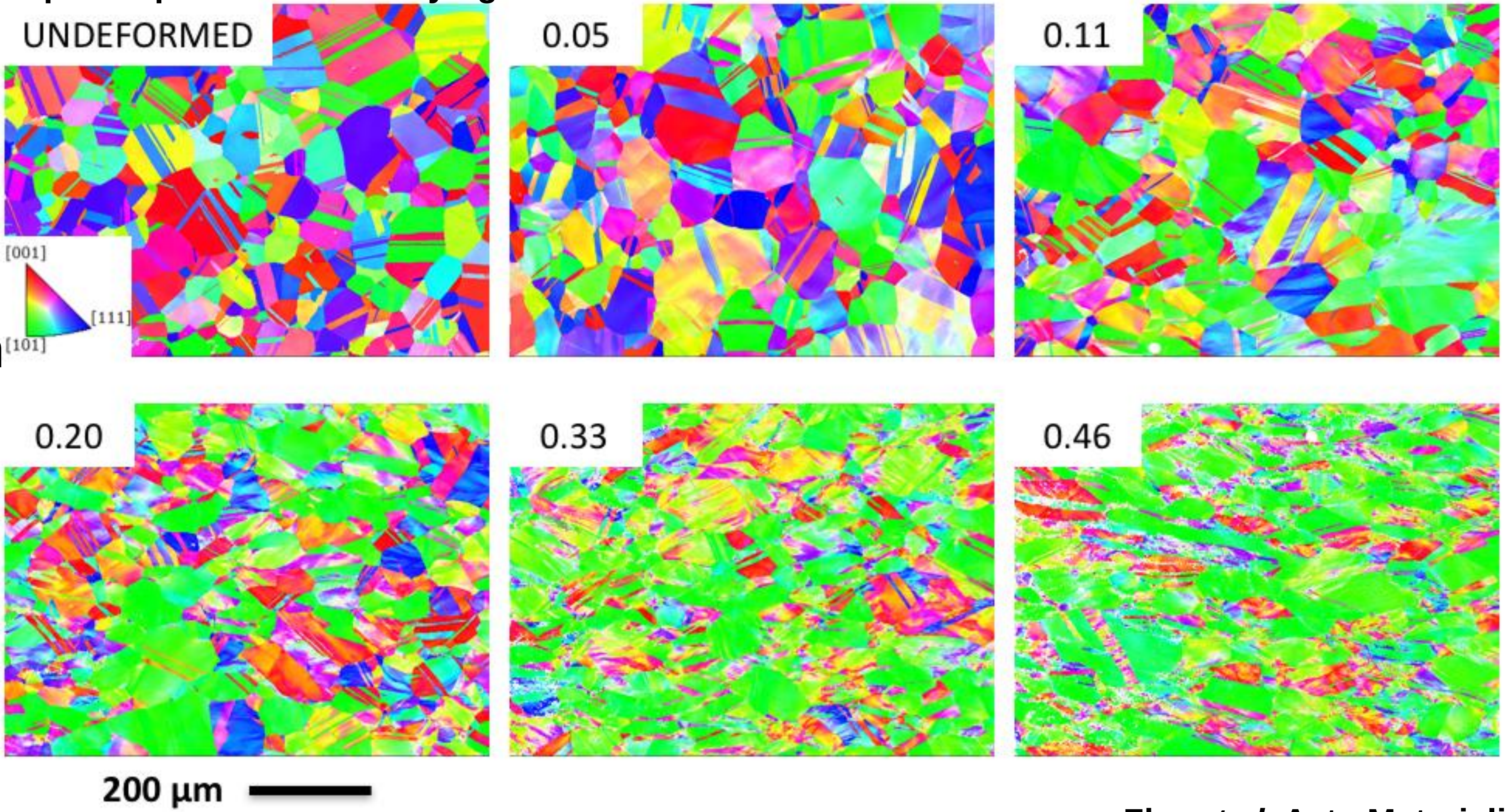

Compression Direction

Zhu *et al*, Acta Materialia, 2018

Deformation Heterogeneity

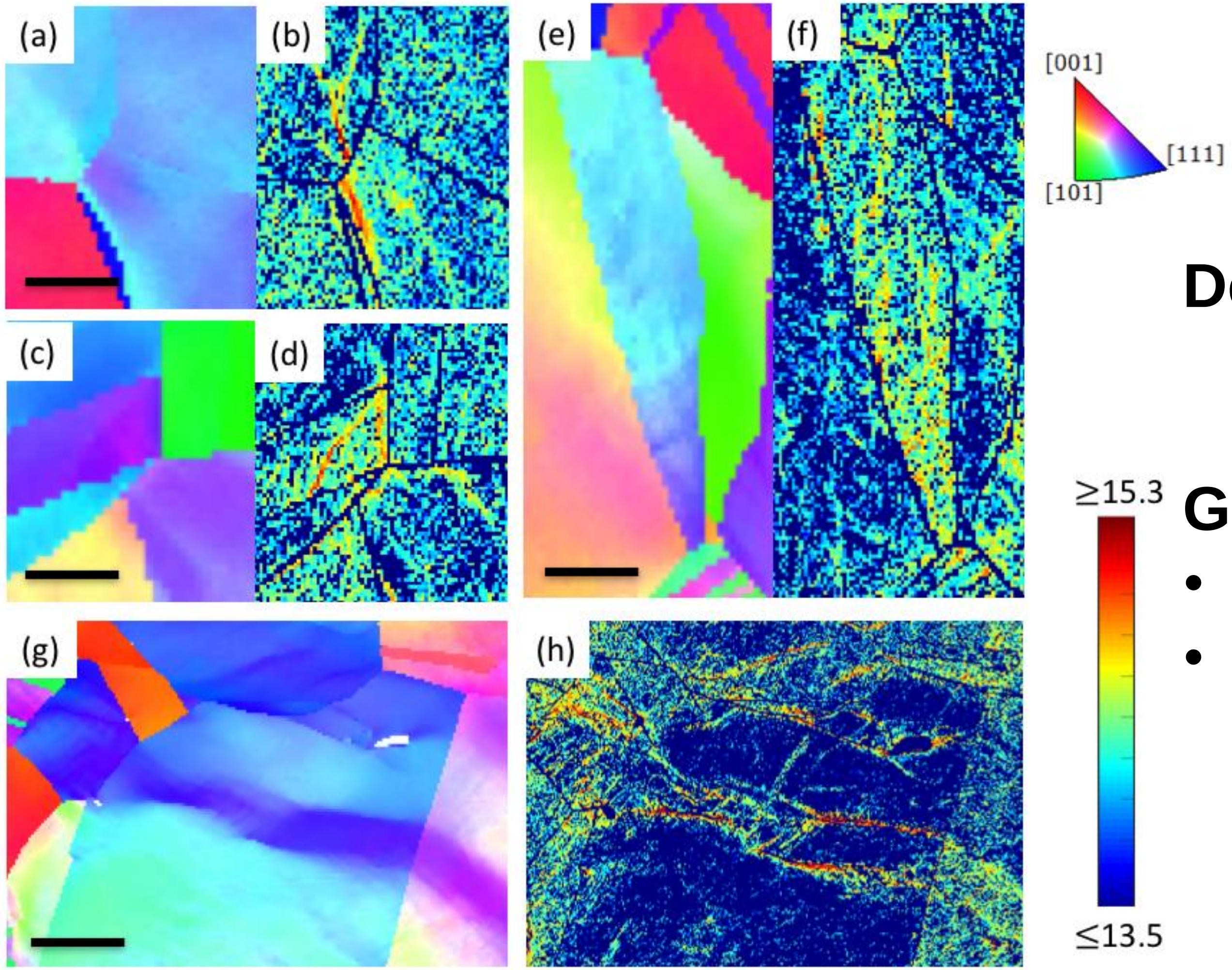

10 µm

Zhu *et al*, Acta Materialia, 2018

Deformation is highly heterogenous

GND hot spots

- Geometric constraint (b)(d)(f)
- Orientation constraint (h)

GND Density Data Distribution

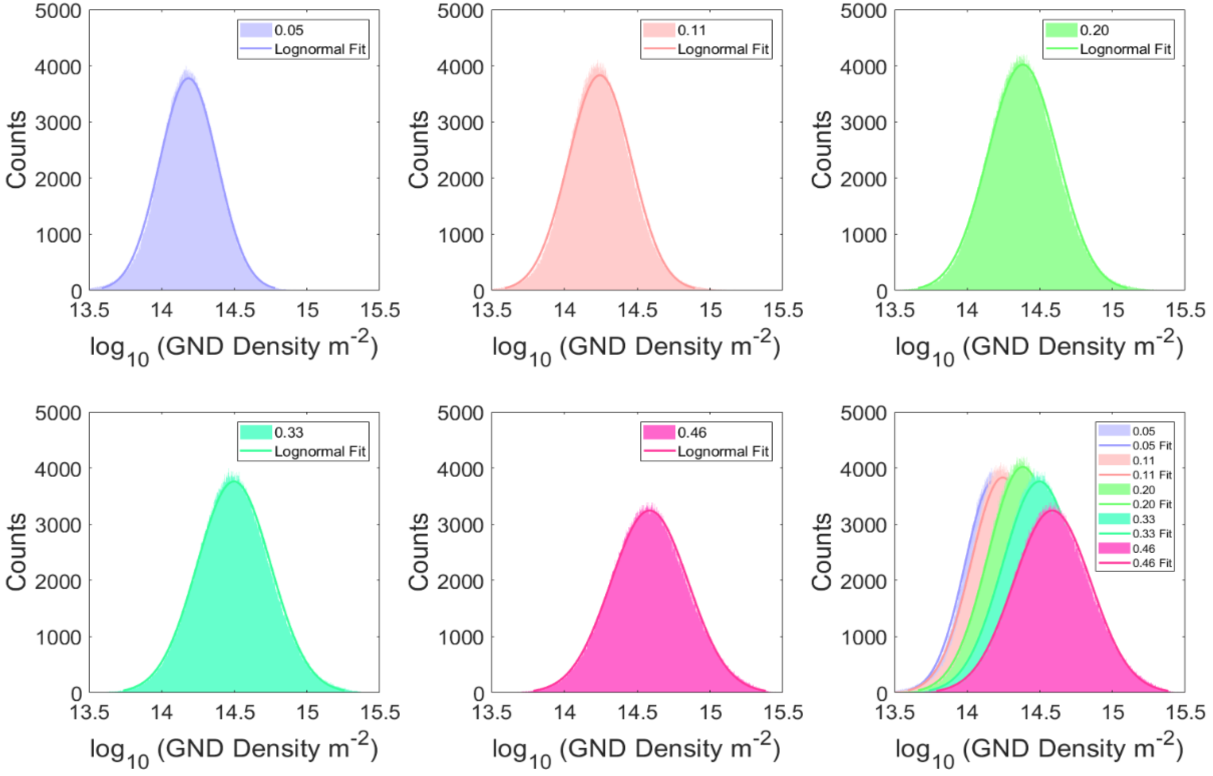

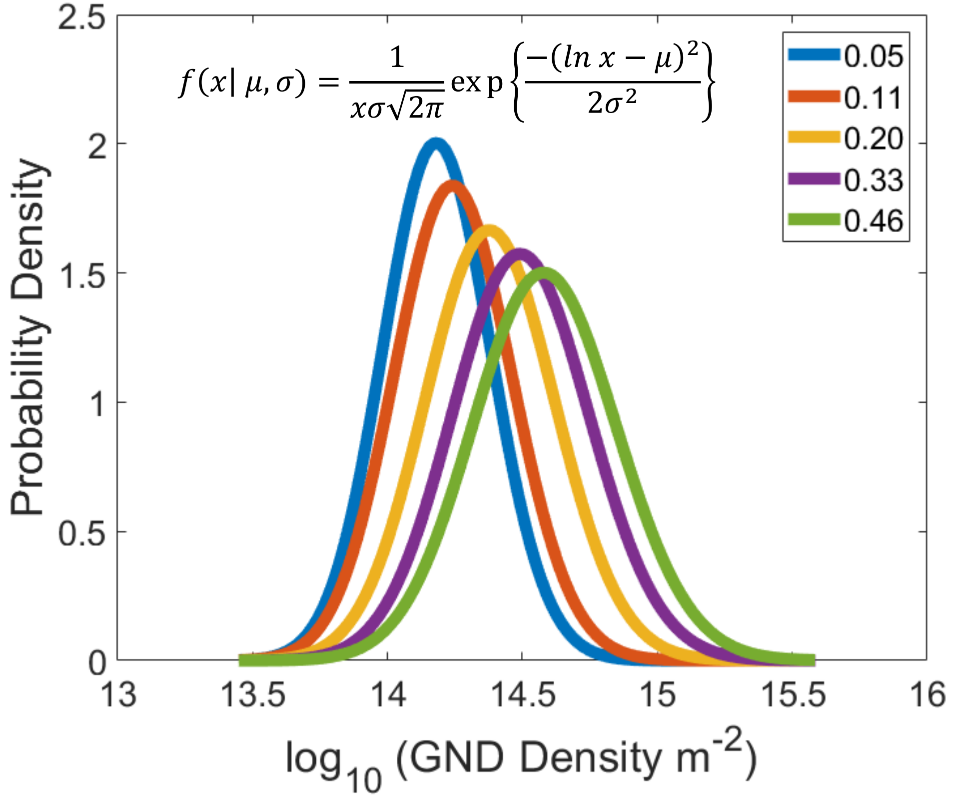

Zhu *et al*, Acta Materialia, 2018
Jiang et al, Acta Materialia, 2013

Consequences of higher applied plastic strain:
1. higher average GND density (↑mean).
2. more heterogenous dislocation distribution (↑ variance).

Ashby and Measured GND Comparison

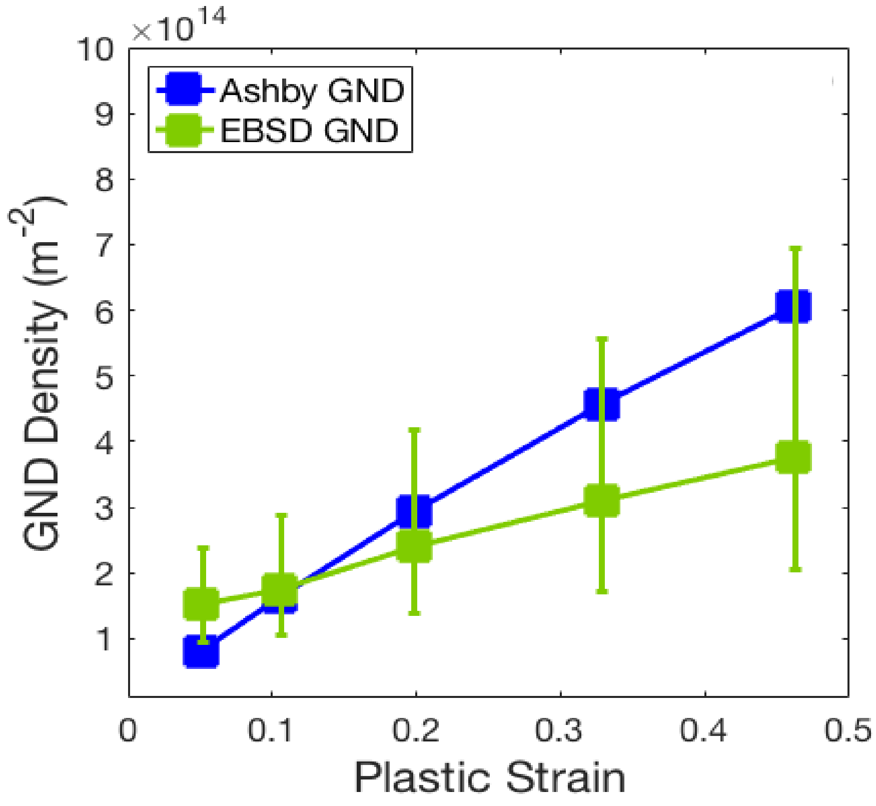

Ashby's Model		Measured GND
Linearity between 0.05 and 0.46		Linearity between 0.05 and 0.46
Rate of increase	>	Rate of increase

Ashby' model predicts the high GND density structures whereas measured GND density covers a wider range of dislocation densities.

Zhu *et al*, Acta Materialia, 2018

Taylor's Hardening Model

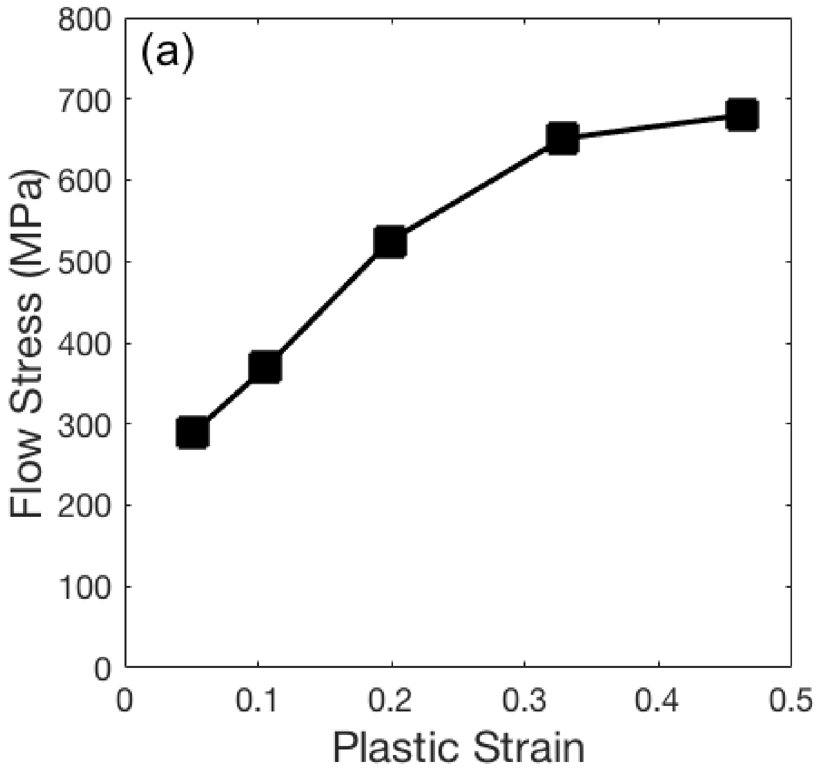

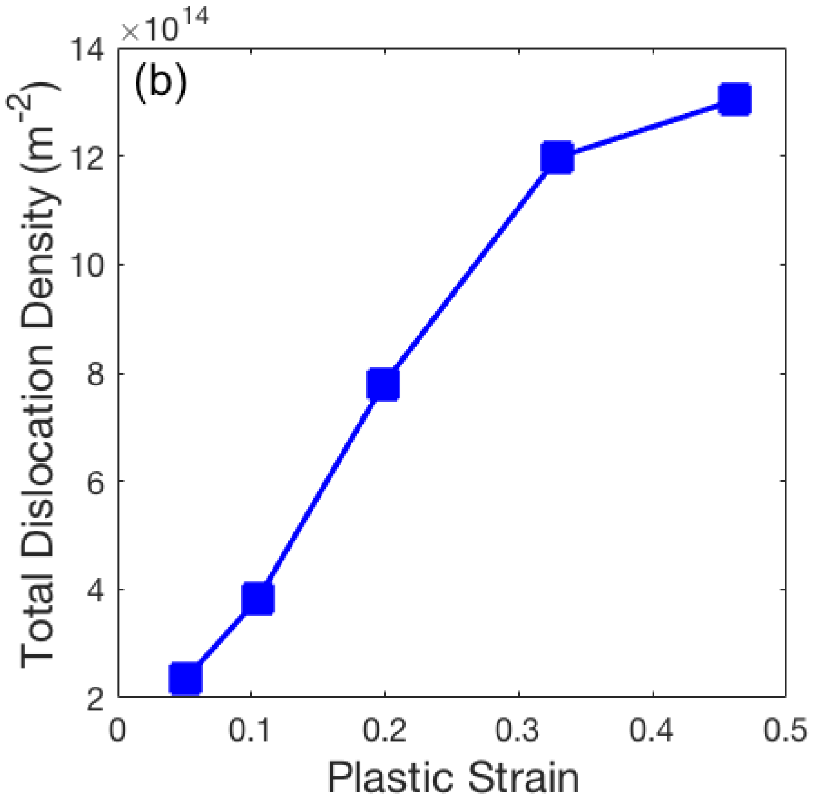

Zhu *et al*, Acta Materialia, 2018

$$\sigma_{flow} = \bar{m}\tau = \bar{m}cGb\sqrt{\rho_T}$$

$$\rho_T = \frac{{\sigma_{flow}}^2}{(\bar{m}cGb)^2}$$

$$\rho_{SSD} = \rho_T - \rho_{GND}$$

Frictional stress in FCC is negligibly small ($\tau_0 = 0$) ;
$\bar{m}$: Taylor's factor;
c: 0.3;
G: shear modulus;
b: Burgers vector

Taylor, 1938
Kubin and Mortensen, 2003
Jiang *et al*, 2013

Dislocation Type Evolution @ R.T.

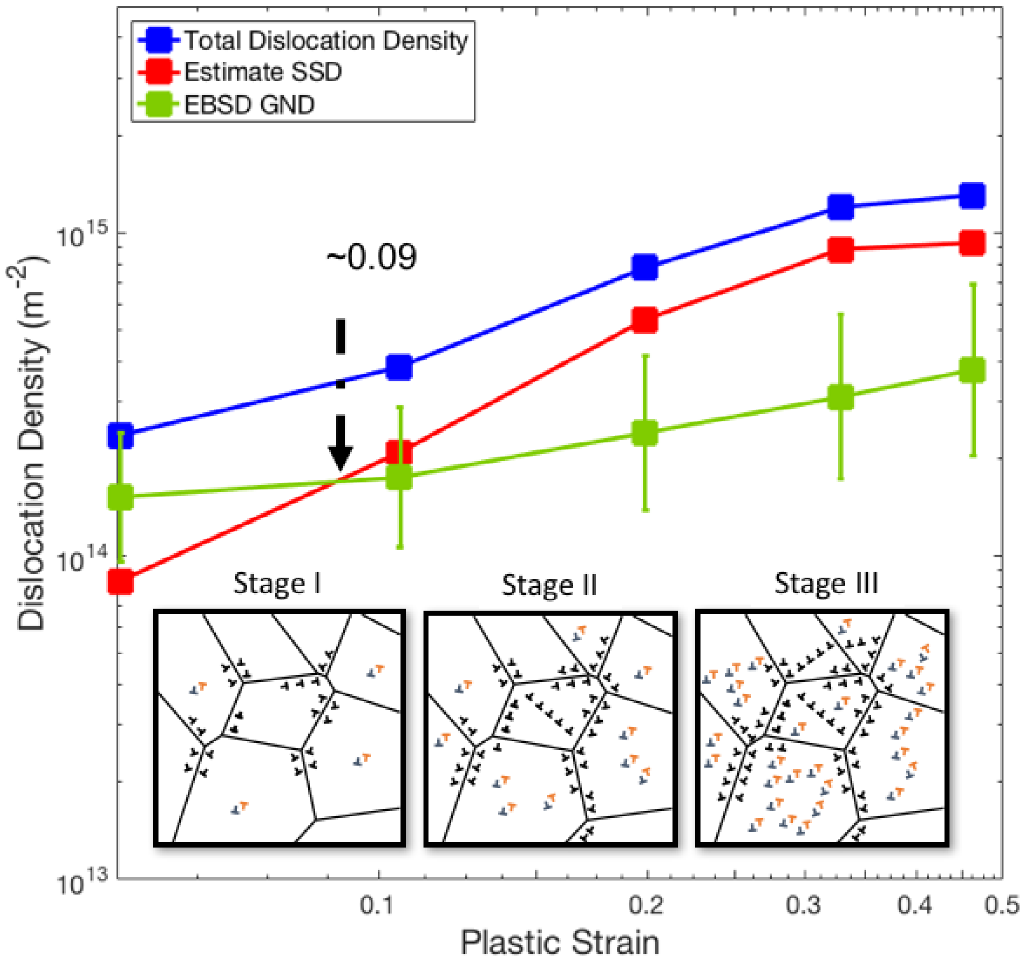

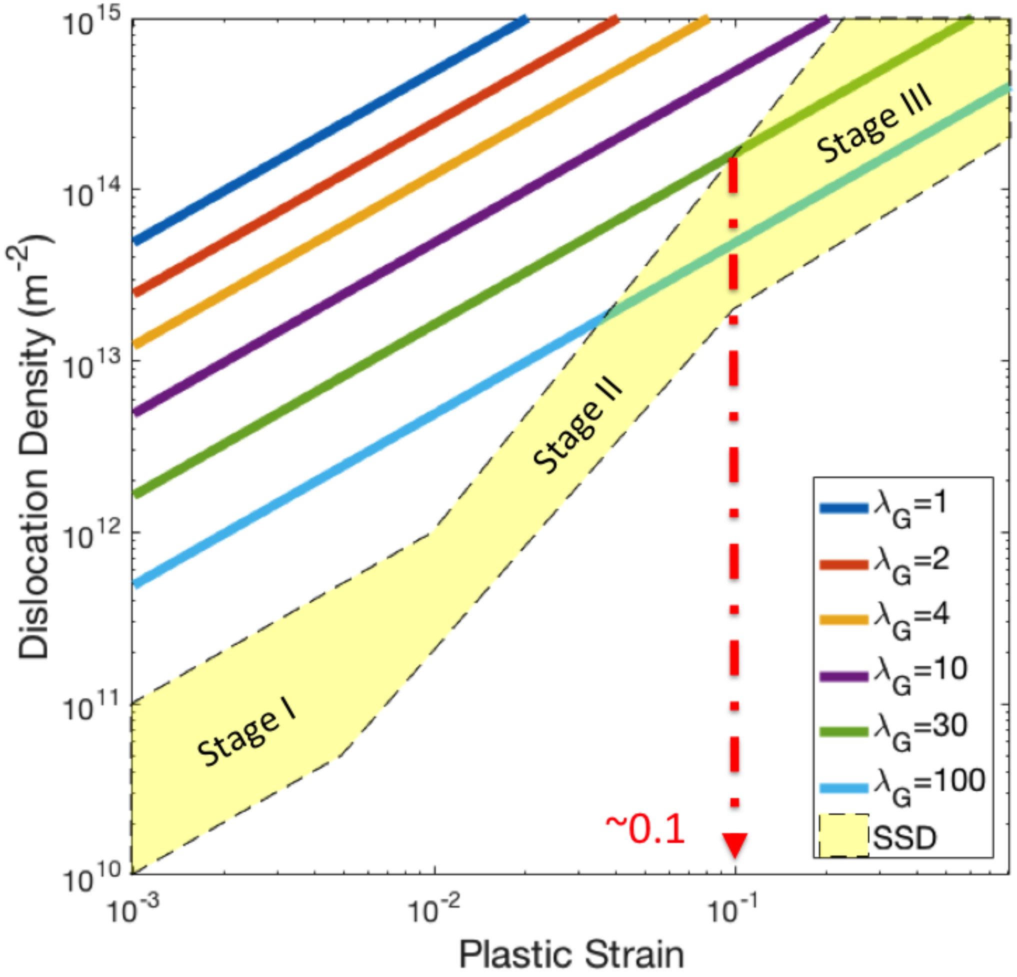

Zhu *et al*, Acta Materialia, 2018

Low strain, GNDs dominated; Higher strain, swamped by SSDs

Future Directions

- Lower strain<0.05 (HR-EBSD)
- Grain size effect
- Temperature effect
- Strain rate effect
- Change materials

Thank you

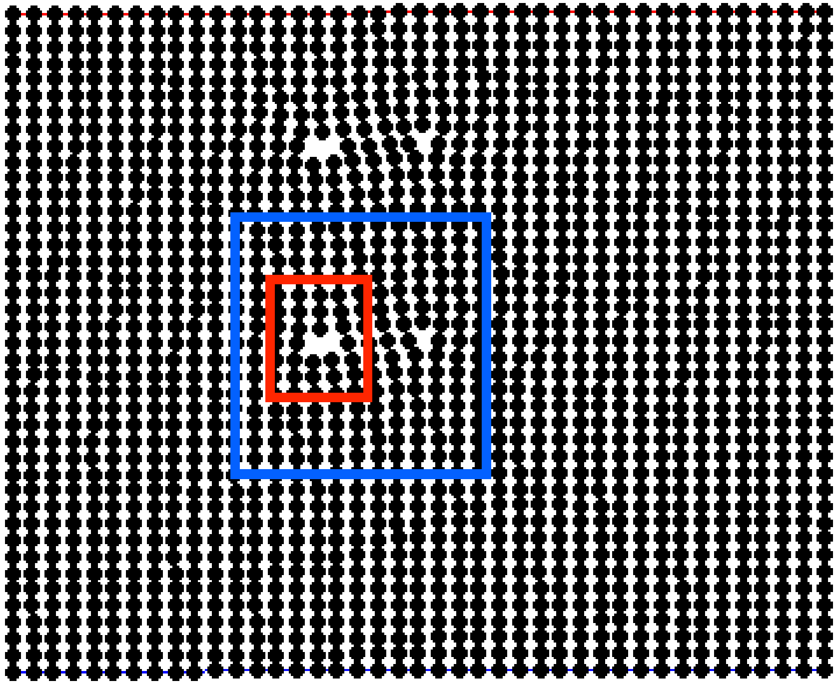

Effect of varying step size

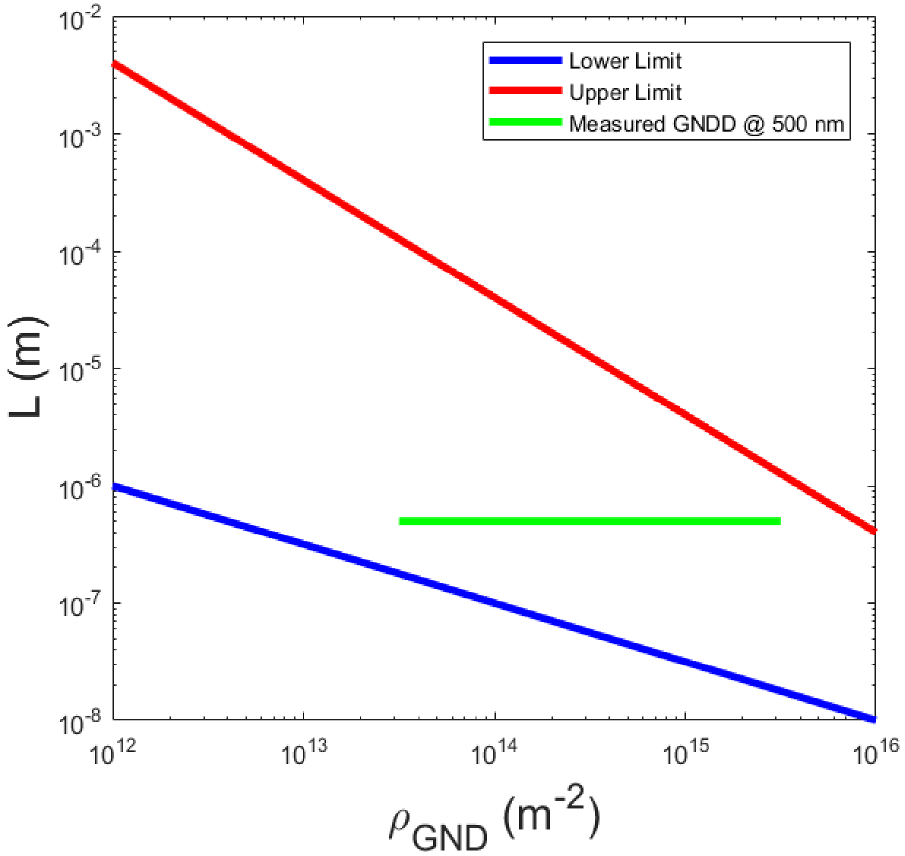

Appropriateness of Step Size